analytical chemistry

Article

pubs.acs.org/ac

A Barcode-Free Combinatorial Screening Platform for Matrix Metalloproteinase Screening

Tushar D. Rane,[†,§] Helena C. Zec,[†] and Tza-Huei Wang*[,†,‡]

[†]Department of Biomedical Engineering and [‡]Department of Mechanical Engineering, Johns Hopkins University, Baltimore, Maryland 21218, United States

Supporting Information

ABSTRACT: Application of droplet microfluidics to combinatorial screening applications remains elusive because of the need for composition-identifying unique barcodes. Here we propose a barcode-free continuous flow droplet microfluidic platform to suit the requirements of combinatorial screening applications. We demonstrate robust and repeatable functioning of this platform with matrix metalloproteinase activity screening as a sample application.

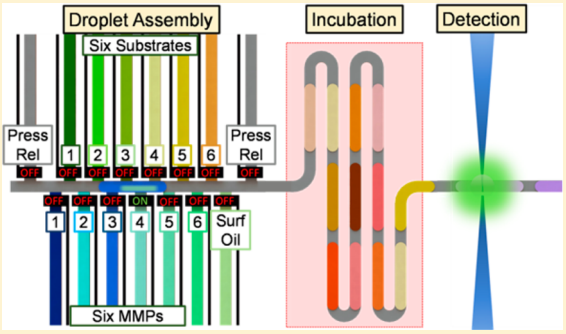

Matrix metalloproteinases (MMPs) make up a family of enzymes involved in a plethora of biological functions. Through their interactions with biological molecules like proteinases, latent growth factors, cell-surface receptors, growth factor binding proteins, etc., they are able to regulate a number of biological processes.[1] Furthermore, this family also plays an important role in pathological conditions like cancer, arthritis, psoriasis, pulmonary emphysema, and endometriosis.[2] It is critical to infer the presence of particular subtypes of the MMP family in biological samples to improve our understanding of their role in pathological processes. Short FRET peptide substrates can be used to sense MMPs through their cleavage activity. However, their relative nonspecificity demands sophisticated mathematical techniques like proteolytic activity matrix analysis (PrAMA)[3] to infer the presence of a specific set of MMPs based on the cleavage signature of an unknown biological sample against a panel of FRET peptide substrates. Techniques like this require large data sets of individual purified MMP cleavage signatures against a large panel of peptide substrates, which can be extremely costly and time-consuming. For instance, screening 10 different MMPs against 10 different substrates at 10 different concentrations of MMPs and substrates each requires testing of 10000 MMP−substrate compositions. Assuming screening in a 96-well plate format and a conservative estimate of 5 h per plate for reaction assembly and data collection, testing 10000 MMP−substrate combinations will require approximately 22 days of continuous processing.

Droplet microfluidics holds tremendous promise for high-throughput biochemical analysis and screening. The power of droplet microfluidics is evident from the scientific literature harnessing this versatile platform for a variety of applications like single-cell analysis,[4−7] single-molecule analysis,[8−11] particle generation,[12] and enzyme kinetics analysis.[13] This technology has really matured in digital analysis of individual biological samples at the single-molecule level.[8,9,14] However, the potential of this technology to address the needs of combinatorial screening applications by replacing standard biochemical assays conducted in a multiwell plate format (microliter regime) to the droplet format (nanoliter to picoliter regime) remains restricted.

A variety of droplet-based schemes for combinatorial screening applications have been proposed. One of the proposed schemes utilizes high-speed electrocoalescence of a reagent droplet library with sample droplets for high-throughput screening of single cells.[4] Despite high-speed operation, this scheme is practically restricted to a small number of reagent−sample combinations (eight combinations reported here) because of the need for a composition-identifying barcode and the limited capability of the barcoding techniques that can be applied to the droplet platform. Furthermore, the reagent and sample droplet volumes are fixed, resulting in a fixed sample:reagent ratio in each droplet. This restriction implies that the reagent droplet library needs to include a population of reagent droplets corresponding to every single discrete reagent concentration to be tested. Another scheme provides an alternative through picoinjection technology. This technology is capable of injecting small quantities of individual reagents into droplets at high speeds. However, picoinjector technology is also limited by the need for droplet barcodes.[15] Picoinjector technology has been applied to MMP screening against FRET substrates.[16] However, because of the

Received: November 16, 2014
Accepted: December 28, 2014
Published: December 28, 2014

DOI: 10.1021/ac504330x
Anal. Chem. 2015, 87, 1950−1956

limitations discussed above, the multiplexing capacity of these demonstrations is limited to a small number of unique MMP−substrate combinations (nine unique compositions reported here), albeit with large number of repeats of each condition.

In this work, we develop a device addressing the issues with the existing droplet-based schemes for combinatorial screening applications. This device is capable of high-throughput matrix metalloproteinase screening without the need for droplet barcodes. This device is based on valve-based droplet generation technology,[17−21] which combines the control offered by microfluidic valves with the high-throughput capacity of droplets. Barcode-free, continuous flow operation of this strategy implies unlimited potential screening capacity on a single device with precise composition control over each individual droplet.

EXPERIMENTAL SECTION

Materials. We used a "MMP Substrate Sampler kit" (Anaspec, Inc., catalog no. 71170) as a source of MMP substrates for our experiments. This kit consists of 16 substrates (SB1−SB16), all of which consist of short peptide sequences labeled with the fluorophore 5-FAM and quencher QXL 520. The exact sequences of peptides from this kit included in our experiments are listed in section 2 of the Supporting Information. The kit also included a fluorescence reference standard (5-FAM-Pro-Leu-OH), which was used to generate standard curves correlating fluorescence intensity with substrate concentration. A "Matrix Metalloproteinase (MMP) Multipack-1" (Enzo Life Sciences, catalog no. BML-AK013-0001) was used as a source of MMPs for our experiments. This kit consists of active recombinant MMP catalytic domains. We used the fluorescent dyes Alexa Fluor 350, Alexa Fluor 488, and Alexa Fluor 647 (Life Technologies) as indicator dyes for the experimental results shown in Figure 2. The input concentrations of these three dyes used for experimental results in Figure 2 were 25, 10, and 10 μM, respectively. Alexa Fluor 546 was used in the form of an oligo labeled with the dye as an indicator dye for our experiments including this dye. All the reagents including fluorescent dyes were diluted to the required concentrations with the reaction buffer included with the MMP substrate sampler kit. BSA (10 μg/mL) was added to the reaction buffer to prevent adsorption of reagents to the device and tubing walls. The oil phase for our experiments consisted of FC-40 (3M) and 1*H*,1*H*,2*H*,2*H*-perfluoro-1-octanol (Sigma-Aldrich) [4:1 (v/v)]. The surfactant oil phase consisted of FC-40 with 2% fluorosurfactant (RAN Biotechnologies) by weight.

Input Reagent Concentrations for Various Experiments. (1) The input dye concentrations used for the image in Figure 2 were 25 μM Alexa Fluor 350, 10 μM Alexa Fluor 488, and 10 μM Alexa Fluor 647. Four different concentrations of these dyes generated in droplets from each of these inputs were 0*X*, 0.1*X*, 0.2*X*, and 0.3*X*, where *X* is the original input concentration of each dye.

(2) The input dye concentrations used for data in Figure 3 were 50 nM Alexa Fluor 488 and 50 nM Alexa Fluor 546. Five different concentrations of each dye apparent in droplet format from Figure 3 were 0*X*, 0.1*X*, 0.2*X*, 0.3*X*, and 0.4*X*, where *X* is the original input concentration of each dye.

(3) For the experimental results in Figures 4 and 5, the input concentration of all MMPs was 5 ng/μL while the concentration of all substrates was 5 μM. The 1*X* MMP concentration in droplets for these figures refers to 1 ng/μL, while the 1*X* substrate concentration refers to 1 μM.

(4) For the experimental results in section 5 of the Supporting Information, the input concentration of all MMPs was 7.5 ng/μL while the concentration of all substrates was 7.5 μM. The 1*X* MMP concentration in droplets for these results refers to 1 ng/μL, while the 1*X* substrate concentration refers to 1 μM.

(5) For the experimental results in Figure 6, the input concentration of all MMPs was 7.5 ng/μL while the concentration of all substrates was 7.5 μM. The 1*X* MMP concentration in droplets for these results refers to 0.5 ng/μL, while the 1*X* substrate concentration refers to 0.5 μM. For each reagent (i.e., MMP and substrate), five different concentrations (1*X*, 2*X*, 3*X*, 4*X*, and 5*X*) were generated on the device.

Experimental Protocol. *On-Chip Experiments.* A set of solenoid valves was used to control the on/off status of the valves on the device. Initially, all the reagent inputs on the device were primed with the respective reagent. Any residual reagents in the central channel following this process were flushed out using the oil phase. Following this, the valve actuation sequence corresponding to the reagent combinations to be generated on the device was executed by a computer. The valve actuation sequence for each droplet consisted of the following steps: (1) buffer droplet generation, (2) droplet displacement in front of other reagent inputs for reagent injection, (3) droplet displacement to the incubation region through injection of the oil phase in the central channel, (4) further displacement of the droplet in the incubation channel through injection of a surfactant oil phase in the central channel, and (5) closing all valves on the device for dissipation of pressure in the central channel. After the proper operation of the device on a microscope had been ensured, the device was moved to a fluorescence detection setup. The fluorescence detection setup we used for our experiments is capable of dual-channel excitation (488 and 552 nm) as well as dual-band detection (506−534 and 608−648 nm). The detection volume of the fluorescence detection setup was placed at the detection region of the device for continuous sensing of fluorescence from droplets passing through that region. The device was maintained at room temperature for all the experiments.

Off-Chip Experiments. For off-chip experimental results used in Figure 5 and Figure S3 of the Supporting Information, MMP and substrate concentrations identical to those being compared in the droplet format were generated in 20 μL reaction mixtures in a 96-well plate format. The fluorescence from the 96-well plate with these reaction mixtures was then monitored on a CFX96 real-time PCR detection system (Bio-Rad Laboratories, Inc.).

Data Analysis of On-Chip Experiments. Fluorescence data obtained from droplet sequences generated on chip were further processed through custom software written in Matlab. This software identified various droplets in a data trace and generated various statistics obtained from the data collected from each droplet. The average droplet fluorescence intensity identified by this software for each droplet was then used to estimate MMP activity rates shown in Figure 5 and Figure S3 of the Supporting Information. Each repeat of a droplet sequence consisted of a substrate-only control for each substrate type and concentration. The average fluorescence intensity of a substrate-only control droplet was subtracted from the average fluorescence intensity of a MMP−substrate combination droplet (with the same substrate concentration), and this intensity difference was converted to a substrate concentration difference using the standard curve in section 4 of the

DOI: 10.1021/ac504330x
Anal. Chem. 2015, 87, 1950−1956

Supporting Information. The substrate concentration difference thus obtained was then divided by the droplet transit time on the device (~12 min) to estimate MMP activity rates for that particular MMP−substrate combination.

Data Analysis of Off-Chip Experiments. For a fair comparison between on-chip and off-chip experiments, the MMP activity rate was estimated from off-chip experiments in a manner similar to that of on-chip experiments. The fluorescence intensity reading from a substrate-only control sample was subtracted from that of a MMP−substrate combination reaction for the same substrate concentration at the same time point (12 min after injection of the enzyme into the reaction mixture). The difference in fluorescence intensities was again converted to the substrate concentration difference, using the standard curve for off-chip experiments in section 4 of the Supporting Information. This substrate concentration difference was then divided by the time for which the enzyme was added to the reaction mixture (12 min) to estimate the MMP activity rate for that particular MMP−substrate combination.

RESULTS AND DISCUSSION

A schematic of the device we designed for this application is illustrated in Figure 1. The device features a central channel with an oil phase input at the upstream end, followed by a reagent injection region, an incubation region, and a fluorescence detection region as one moves downstream. The device also has 12 individual reagent inputs. We also included "pressure relief" channels on this device, to decouple the dependence of droplet size generated on the device from the changing flow resistance of the incubation region. The valves corresponding to the pressure relief channels are opened during reagent injection and droplet displacement operations on the device.

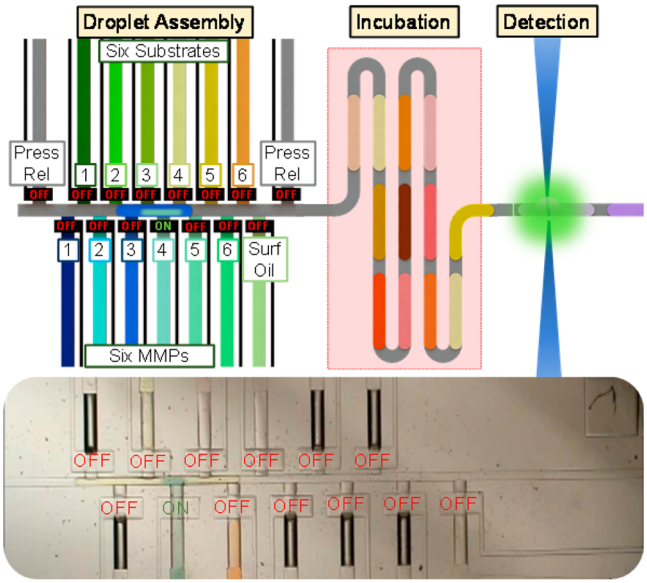

Figure 1. MMP screening platform. In step 1, droplet assembly through a microfluidic valve (thin black channels) controlled injection of desired MMP(s) and substrate(s) in a buffer droplet. Step 2 is incubation of assembled MMP−substrate droplets in the incubation channel on the device. Step 3 is serial interrogation of droplets through confocal fluorescence spectroscopy while preserving the order of generation, precluding the need for a barcode to identify the composition of each droplet (Press Rel, pressure relief channels; Surf Oil, surfactant oil input described in the text). The image at the bottom shows the droplet assembly region on an actual microfluidic device.

The device operation sequence is illustrated in Figure 1. The most upstream reagent input is dedicated to dispensing reaction buffer into droplets. For every droplet generated on the device, initially a buffer droplet is dispensed in the central channel. As all reagents are constantly maintained under pressure, opening the valve for a particular reagent results in release of a reagent droplet into the central channel. The valve opening time as well as the pressure magnitude applied to the reagents can be used to control the volume of the reagent dispensed into the central channel. After this mechanism is used to dispense a buffer droplet, this droplet is moved in front of the input corresponding to the next reagent to be injected, using a flow of the oil phase from the oil input to the central channel, and the injection of the next reagent is completed. This sequence of steps can be repeated as many times as desired to inject up to 12 reagents in each droplet using this device. After a complete reaction mixture droplet is assembled, this droplet is moved to the downstream incubation region. The length of the incubation region can be modified to achieve the desired incubation time of the droplets on the device. Following incubation, the droplets move to a fluorescence detection region where they are interrogated by a confocal fluorescence spectroscopy system for the reaction outcome. Figure 1 also shows an image of the droplet generation region on an actual device. All three steps of device operation can be seen in movies in the Supporting Information. This scheme of combinatorial droplet generation has a few salient features that set it apart from other droplet microfluidic platforms described above. Under this scheme, up to 12 different reagents can be injected into a reagent droplet at various independently controlled proportions. The device can operate in a completely automated manner through execution of a predetermined valve actuation sequence. This automation also implies that various reaction mixtures can be generated in a predetermined order as desired. This feature also provides the device with the ability to generate exactly as many repeats of a reaction mixture as desired. Simultaneous operation of all three steps, i.e., droplet generation, incubation, and fluorescence detection, implies that this device has virtually unlimited screening capacity. Even at a very conservative estimate of 10 different reagent concentrations for each reagent in a droplet, a single device is capable of producing 1 trillion different droplet compositions. Most importantly, because the order of droplets is maintained throughout the device, droplets are automatically spatially coded, precluding the need for composition-identifying unique barcodes.

We designed a microfluidic device to execute the workflow proposed in Figure 1. The details of device fabrication can be found in section 1 of the Supporting Information. The device was then tested for its capability to generate various combinations of input reagents in a predetermined sequence using fluorescent dyes as reagents. In our first test, we generated all possible combinations of four different concentrations of three different fluorescent dyes on our microfluidic device (Figure 2). Each white square in the collage in Figure 2 includes three images of a droplet taken with red, green, and blue filters from top to bottom, respectively (details in the Experimental Section). A progressive sequence of changing droplet compositions can be seen as one moves from left to

DOI: 10.1021/ac504330x
Anal. Chem. 2015, 87, 1950−1956

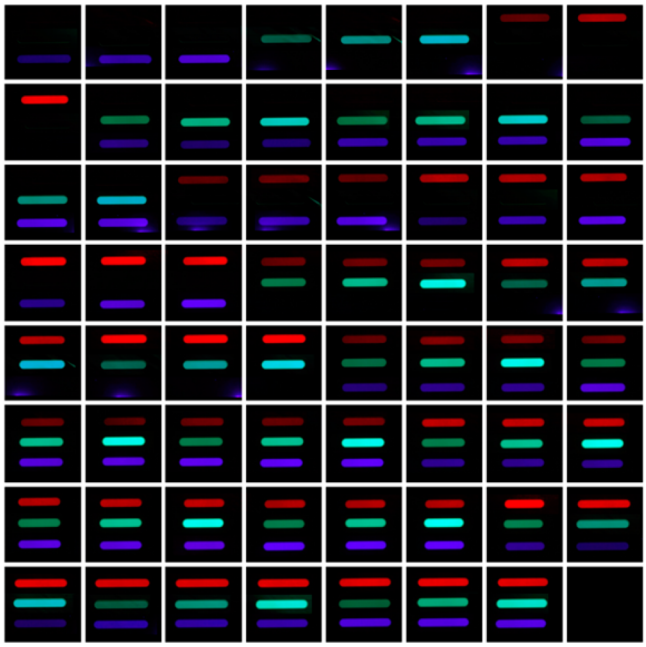

Figure 2. Series of fluorescent droplets generated on a single device. Each white square contains three images of a single droplet collected using DAPI, FITC, and Cy5 filter sets on a fluorescence microscope from the bottom to top, respectively. The droplets represent all possible combinations of four different intensities of three different fluorescent dyes (Alexa Fluor 350, Alexa Fluor 488, and Alexa Fluor 647) generated on the device.

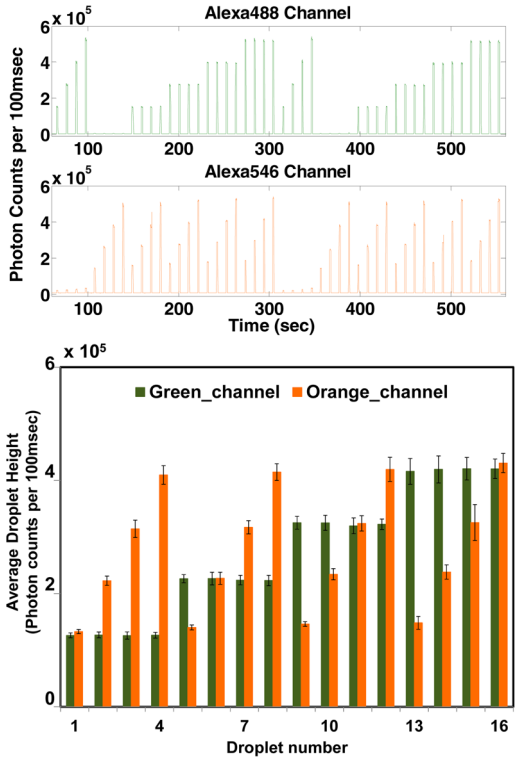

Figure 3. Droplet composition control and serial droplet fluorescence detection on the device. The two data traces show two repeats of a sequence of 24 droplets generated on the device. The green trace indicates fluorescence from the Alexa Fluor 488 channel (506−534 nm), while the orange trace indicates fluorescence from the Alexa Fluor 546 channel (608−648 nm). The fluorescence data indicate the capability of the device to independently control the concentration of different reagents in individual droplets. The bar plot on the bottom indicates the average fluorescence intensity of droplets with both dyes in the sequence. The error bars indicate the standard deviations in average fluorescence intensity over 10 repeats of the sequence.

right in each row, beginning with increasing concentrations of individual dyes followed by all combinations of pairs of dyes followed by all combinations of triplets of dyes.

An important characteristic of the combinatorial reaction generation system is the reagent concentration dynamic range of the system. The upper end of this range is fixed by the input reagent concentration. The response time of the valves used in our scheme as well as the minimal pressure that can be applied to a reagent for reliable injection puts a lower limit on the smallest reagent volume that can be injected into a droplet. However, this limitation theoretically does not limit the lower end of the reagent concentration dynamic range as the buffer droplet size can always be made as large as necessary to achieve the required concentration. Practically, however, we observed that large volume droplets because of their large lengths tend to break up during transit through the incubation region on the device. Given these constraints, we were able to achieve a maximal dilution of 6 parts per 1000 on our device (details in section 3 of the Supporting Information). This number, however, is limited to our current device design as well as the oil−surfactant system used in our experiments. An increase in channel height in the incubation region, to decrease droplet length, as well as the choice of a modified oil−surfactant system for better droplet stability may further reduce the dilution limit we were able to achieve without causing droplet breakup on our device. Furthermore, as indicated in Figure S1 of the Supporting Information, the fluorescence intensity of a reagent (and hence the reagent injection volume) in a droplet varies linearly with valve opening time. This allows for precise reagent injection control in each individual droplet through simple predetermined valve opening time calculation. Figure 3 demonstrates this capability of the device through independent control of the concentration of two different fluorescent dyes in droplets via automated execution of a predetermined valve actuation sequence. We then tested the applicability of our droplet system for screening of MMPs against a variety of peptide substrates on our device for their specificity and activity. The peptide substrates used are short peptide sequences labeled with a fluorophore (5-FAM) and a quencher (QXL 520) on either end. In the presence of an MMP, the peptide sequence is cleaved, resulting in separation of the fluorophore from the quencher and a consequent increase in the fluorophore's fluorescence. The rate of increase in fluorescence of an MMP−substrate sample can then serve as a proxy for the activity of the MMP against the peptide substrate.

Figure 4 shows data traces obtained from two repeats of a droplet sequence containing various combinations of MMPs and substrates. The data trace in the top panel indicates the fluorescence emitted by the fluorophore on the peptide substrates. However, for a droplet sequence with an unknown outcome (as opposed to a fluorescent dye dilution series), it can be difficult to estimate the position of each droplet in the whole long sequence and to ensure that the device is operating robustly without any unwanted merging or breakup of droplets. Therefore, we also included some "beacon" droplets in the droplet sequence, generated through different dilutions of a fluorescent dye different from the fluorescent dye on the MMP

DOI: 10.1021/ac504330x
Anal. Chem. 2015, 87, 1950−1956

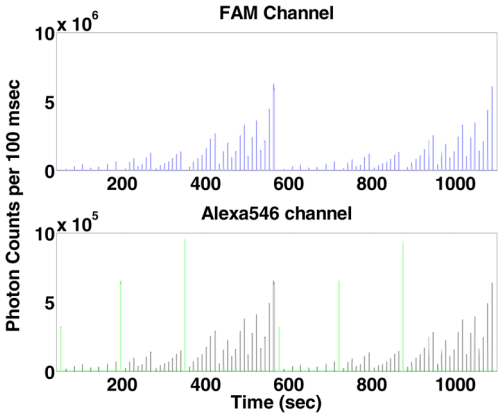

Figure 4. MMP−substrate assay on the device. The two data traces indicate fluorescence obtained from two repeats of a sequence of droplets containing different MMP−substrate combinations. The FAM channel indicates fluorescence from the FRET peptide substrates cleaved by different MMPs. Alexa Fluor 546 dye is used to insert a few "beacon" droplets (green peaks in the Alexa Fluor 546 channel) into the droplet sequence without interfering with the assay channel. The presence of beacon droplets in the sequence at predetermined positions with respect to other droplets can be used as an indicator of the proper operation of the device without any unwanted droplet merging or splitting. The fluorescence from the nonbeacon droplets in the Alexa Fluor 546 channel is due to bleeding of some fluorescence from the FAM channel into the Alexa Fluor 546 channel.

substrates. These droplets are indicated in the data trace from the Alexa Fluor 546 channel. The known repeating pattern of these droplets allows us to easily discern repeats of a droplet sequence from the data. Furthermore, their predetermined location in the droplet sequence allows us to ensure that the device is operating in a robust manner without any unwanted merging or breakup of droplets as any unwanted merging or breakup would result in a change in the position of a beacon droplet in the whole sequence. It should be noted that these beacon droplets are not limited by different fluorescence intensities that can be easily distinguished by the detection system similar to fluorescence intensity-based barcodes used in other droplet-based combinatorial schemes described earlier. The possibility of varying intensities, varying counts, and varying spacing between beacon droplets provides for virtually unlimited possible beacon droplets marking different positions in an extremely long droplet sequence.

We then compared the substrate cleavage rates for various MMP−substrate combinations we observed on our device against cleavage rates we observed in off-chip experiments. Some representative results are shown in Figure 5, while others are included in section 5 of the Supporting Information. Our comparison indicates that the cleavage rates of enzymes MMP1, MMP2, and MMP9 matched across platforms fairly well for various substrates. However, the substrate cleavage rates for MMP8 and MMP13 were consistently low on the device when compared with cleavage rates in off-chip experiments. Interaction of proteins with the oil−surfactant system used in droplet devices has been reported in the literature.[22,23] Our results indicate that the oil−surfactant system we used interacts with MMP8 and MMP13, reducing their activity. Some

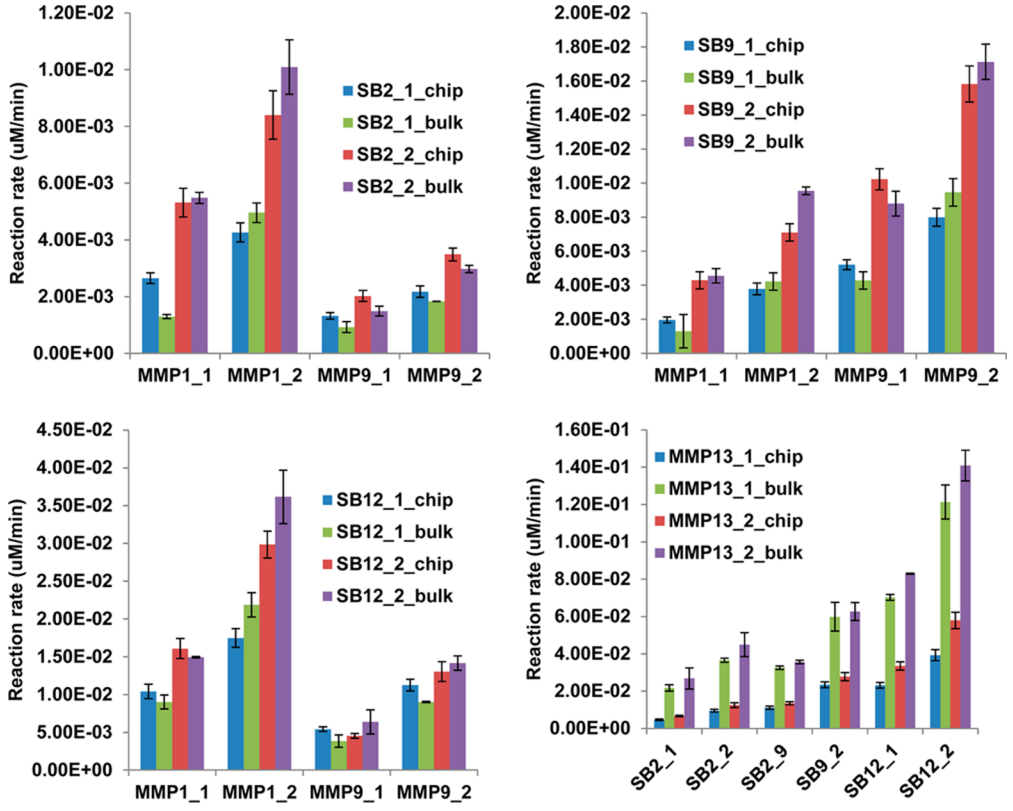

Figure 5. MMP activity comparison between on- and off-chip experiments. The cleavage rates of different MMP types against different substrates estimated from corresponding droplets on the device are compared to cleavage rates estimated for the same reaction conditions from off-chip experiments: MMP1_1, MMP1 at a 1*X* concentration; SB9_2_chip, substrate SB9 at a 2*X* concentration on-chip; SB12_1_bulk, substrate SB12 at a 1*X* concentration off-chip.

DOI: 10.1021/ac504330x
Anal. Chem. 2015, 87, 1950−1956

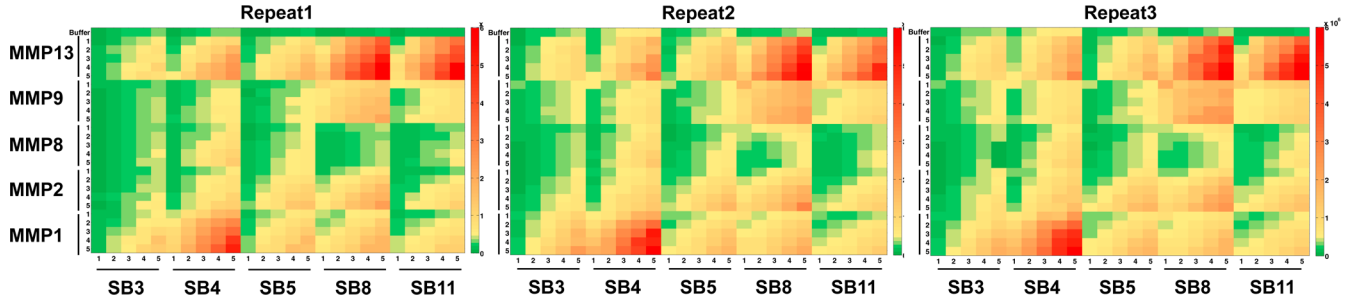

Figure 6. Average measured droplet fluorescence intensities from three repeats of 650 unique MMP−substrate combinations. The labels indicate the corresponding reagent (e.g., SB3, MMP1, etc.). For each reagent, five different concentrations were tested. For each MMP, the concentration increases from top to bottom, whereas for each substrate, the concentration increases from left to right. The top row in each repeat indicates results from a substrate-only control in which no MMPs were used.

solutions have been proposed in the literature to engineer better surfactants with substantially weakened interaction with proteins.[22,23] These solutions can potentially make this platform suitable for a broad range of enzymatic screening. As a proof of principle of screening a large number of enzyme−substrate combinations on a single device, we generated a droplet train consisting of 650 unique droplet compositions (Figure 6, details in the Experimental Section and section 6 of the Supporting Information). The activity patterns from three repeats of this sequence show excellent similarity. We, however, did observe that following long-term operation of the device the hydrophobic treatment wears off, resulting in more sticking of droplet contents to the channel surface. Superhydrophobic treatments have been proposed in the literature to fabricate antifouling surfaces. Integration of these surfaces with our device design can potentially increase the time span for which a device can function without significant channel surface fouling.

CONCLUSION

In summary, we demonstrated a droplet device for combinatorial screening applications without the need for composition-identifying unique barcodes. We expect this format of droplet devices to increase the applicability of droplet microfluidics to applications requiring the capability of rapid heterogeneous reaction generation.

ASSOCIATED CONTENT

Supporting Information

Experimental details and videos demonstrating functioning of the microfluidic device. This material is available free of charge via the Internet at http://pubs.acs.org.

AUTHOR INFORMATION

Corresponding Author

*E-mail: thwang@jhu.edu.

Present Address

[§]T.D.R.: Mork Family Department of Chemical Engineering and Materials Science, University of Southern California, Los Angeles, CA 90089-1211.

Notes

The authors declare no competing financial interest.

ACKNOWLEDGMENTS

We thank our funding agencies, including the National Institutes of Health (R01CA155305 and R21CA173390) and the National Science Foundation (1159771).

REFERENCES

(1) Sternlicht, M. D.; Werb, Z. *Annu. Rev. Cell Dev. Biol.* **2001**, *17*, 463−516.
(2) Amalinei, C.; Caruntu, I. D.; Giusca, S. E.; Balan, R. A. *Rom. J. Morphol. Embryol.* **2010**, *51*, 215−228.
(3) Miller, M. A.; Barkal, L.; Jeng, K.; Herrlich, A.; Moss, M.; Griffith, L. G.; Lauffenburger, D. A. *Integr. Biol.* **2011**, *3*, 422−438.
(4) Brouzes, E.; Medkova, M.; Savenelli, N.; Marran, D.; Twardowski, M.; Hutchison, J. B.; Rothberg, J. M.; Link, D. R.; Perrimon, N.; Samuels, M. L. *Proc. Natl. Acad. Sci. U.S.A.* **2009**, *106*, 14195−14200.
(5) Rane, T. D.; Zec, H. C.; Puleo, C.; Lee, A. P.; Wang, T. *Lab Chip* **2012**, *12*, 3341−3347.
(6) Baret, J. C.; Miller, O. J.; Taly, V.; Ryckelynck, M.; El-Harrak, A.; Frenz, L.; Rick, C.; Samuels, M. L.; Hutchison, J. B.; Agresti, J. J.; Link, D. R.; Weitz, D. A.; Griffiths, A. D. *Lab Chip* **2009**, *9*, 1850−1858.
(7) Zeng, Y.; Novak, R.; Shuga, J.; Smith, M. T.; Mathies, R. A. *Anal. Chem.* **2010**, *82*, 3183−3190.
(8) Hindson, B. J.; Ness, K. D.; Masquelier, D. A.; Belgrader, P.; Heredia, N. J.; Makarewicz, A. J.; Bright, I. J.; Lucero, M. Y.; Hiddessen, A. L.; Legler, T. C.; Kitano, T. K.; Hodel, M. R.; Petersen, J. F.; Wyatt, P. W.; Steenblock, E. R.; Shah, P. H.; Bousse, L. J.; Troup, C. B.; Mellen, J. C.; Wittmann, D. K.; Erndt, N. G.; Cauley, T. H.; Koehler, R. T.; So, A. P.; Dube, S.; Rose, K. A.; Montesclaros, L.; Wang, S.; Stumbo, D. P.; Hodges, S. P.; Romine, S.; Milanovich, F. P.; White, H. E.; Regan, J. F.; Karlin-Neumann, G. A.; Hindson, C. M.; Saxonov, S.; Colston, B. W. *Anal. Chem.* **2011**, *83*, 8604−8610.
(9) Zhong, Q.; Bhattacharya, S.; Kotsopoulos, S.; Olson, J.; Taly, V.; Griffiths, A. D.; Link, D. R.; Larson, J. W. *Lab Chip* **2011**, *11*, 2167−2174.
(10) Rane, T. D.; Puleo, C. M.; Liu, K. J.; Zhang, Y.; Lee, A. P.; Wang, T. H. *Lab Chip* **2010**, *10*, 161−164.
(11) Kumaresan, P.; Yang, C. J.; Cronier, S. A.; Blazej, R. G.; Mathies, R. A. *Anal. Chem.* **2008**, *80*, 3522−3529.
(12) Song, H.; Chen, D. L.; Ismagilov, R. F. *Angew. Chem., Int. Ed.* **2006**, *45*, 7336−7356.
(13) Song, H.; Ismagilov, R. F. *J. Am. Chem. Soc.* **2003**, *125*, 14613−14619.
(14) Baker, M. *Nat. Methods* **2012**, *9*, 541−544.
(15) Abate, A. R.; Hung, T.; Mary, P.; Agresti, J. J.; Weitz, D. A. *Proc. Natl. Acad. Sci. U.S.A.* **2010**, *107*, 19163−19166.
(16) Chen, C. H.; Miller, M. A.; Sarkar, A.; Beste, M. T.; Isaacson, K. B.; Lauffenburger, D. A.; Griffith, L. G.; Han, J. *J. Am. Chem. Soc.* **2013**, *135*, 1645−1648.
(17) Guo, F.; Liu, K.; Ji, X.; Ding, H.; Zhang, M.; Zeng, Q.; Liu, W.; Guo, S.; Zhao, X. *Appl. Phys. Lett.* **2010**, *97*, 233701-3.
(18) Zeng, S.; Li, B.; Su, X.; Qin, J.; Lin, B. *Lab Chip* **2009**, *9*, 1340−1343.
(19) Zec, H.; Rane, T. D.; Wang, T. *Lab Chip* **2012**, *12*, 3055−3062.
(20) Jambovane, S.; Kim, D. J.; Duin, E. C.; Kim, S. K.; Hong, J. W. *Anal. Chem.* **2011**, *83*, 3358−3364.

DOI: 10.1021/ac504330x
Anal. Chem. 2015, 87, 1950−1956

(21) Unger, M. A.; Chou, H. P.; Thorsen, T.; Scherer, A.; Quake, S. R. *Science* **2000**, *288*, 113−116.
(22) Holtze, C.; Rowat, A. C.; Agresti, J. J.; Hutchison, J. B.; Angile, F. E.; Schmitz, C. H.; Koster, S.; Duan, H.; Humphry, K. J.; Scanga, R. A.; Johnson, J. S.; Pisignano, D.; Weitz, D. A. *Lab Chip* **2008**, *8*, 1632−1639.
(23) Roach, L. S.; Song, H.; Ismagilov, R. F. *Anal. Chem.* **2005**, *77*, 785−796.

DOI: 10.1021/ac504330x
Anal. Chem. 2015, 87, 1950−1956